Liquid Crystals
Publication details, including instructions for authors and subscription information:
http://www.informaworld.com/smpp/title~content=t713926090

Synthesis and mesomorphism of 6-Z-n-alkyl-alpha-D-galactopyranoses

P. Bault; P. Gode; G. Goethals; J. W. Goodby; J. A. Haley; S. M. Kelly; G. H. Mehl; P. Villa

Online publication date: 06 August 2010

To cite this Article Bault, P. , Gode, P. , Goethals, G. , Goodby, J. W. , Haley, J. A. , Kelly, S. M. , Mehl, G. H. and Villa, P.(1999) 'Synthesis and mesomorphism of 6-Z-n-alkyl-alpha-D-galactopyranoses', Liquid Crystals, 26: 7, 985 — 997
To link to this Article: DOI: 10.1080/026782999204336
URL: http://dx.doi.org/10.1080/026782999204336

LIQUID CRYSTALS, 1999, VOL. 26, NO. 7, 985–997

Synthesis and mesomorphism of 6-*Z*-*n*-alkyl-α-D-galactopyranoses

P. BAULT, P. GODE, G. GOETHALS, J. W. GOODBY†, J. A. HALEY†,
S. M. KELLY*†‡, G. H. MEHL† and P. VILLA

Laboratoire de Chimie Organique et Cinetique, Faculté de Science,
Université de Picardie Jules Verne, 33 rue Saint-Leu, 80039 Amiens, France
†Department of Chemistry, The University of Hull, Hull HU6 7RX, UK

(*Received 3 December 1998; accepted 16 February 1999*)

Three homologous series of 6-*Z*-*n*-alkyl-α-D-galactopyranoses, where linking group *Z* represents either a carboxy group (OCO), a sulphur atom (S) or a propylthio group (C_3H_6S), have been synthesized starting from 1,2:3,4-di-*O*-isopropylidene-α-D-galactopyranose in two or three steps. The length of the terminal aliphatic chains has been varied systematically and the effect on the thermotropic liquid crystal transition temperatures studied. An enantiotropic smectic A* phase was found for each of the homologues prepared. The order of efficiency of the linking group *Z* in favouring liquid crystal formation for the same homologues of the 6-*O*-*n*-acyl-α-D-galactopyranoses (*Z* = OCO), 6-*S*-*n*-alkyl-6-thio-α-D-galactopyranoses (*Z* = S), 6-*O*-*n*-alkyl-α-D-galactopyranoses (*Z* = O) and 6-*O*-(propylene-[3′-*S*-*n*-alkyl])-α-D-galactopyranoses (OC_3H_6S), is S≈ OCO> O> OC_3H_6S. This correlates well with the order of polarisability of *Z* for the first of the linking groups (*Z* = S, OCO, O). The low clearing point of the 6-*O*-(propylene-[3′-*S*-*n*-alkyl])-α-D-galactopyranoses may be due to the presence of a non-conjugated heteroatom in the terminal aliphatic chain. This has parallels with similar behaviour found for non-amphiphilic liquid crystals and is not well understood.

1. Introduction

Chemically simple carbohydrate derivatives, which exhibit thermotropic liquid crystalline properties in the pure state or lyotropic properties with solvents (especially water), are of increasing interest for a number of reasons. Mixtures of monosaccharides, oligosaccharides and polysaccharides, such as alkyl polyglycosides (APGs), have significant practical applications as non-ionic surfactants, which are non-toxic, biocompatible and biodegradable. They are especially attractive as detergents as they are easily prepared in a high overall yield in tens of thousands of tons p.a. from a diverse, renewable and natural resource. They are used, for example, as cheap components of detergents for laundry and dishwashing applications [1–3]. More expensive, monodisperse monosaccharides, such as alkyl glycosides, are commercially available as mild solvents for membrane proteins, which can be solvated, extracted, separated and reconstituted in their original, non-denatured form [4, 5]. They are also used as the major components of liposomes and vesicles in high-value-added drug release formulations [6, 7], as well as exhibiting promising antiviral and antibacterial activity themselves [8–10]. Perfluorinated carbohydrate derivatives have also been used as artificial blood [11]. Most of these practical applications of carbohydrates involve aqueous solutions, suspensions, emulsions or gels. Since the solubility, surface tension, critical micelle concentration, lyotropic phase formation, aqueous gel formation, etc., are all dependent on the hydrophilic–lipophilic balance (HLB) [12], i.e. on the chain length of the alkyl/acyl substituent for a given carbohydrate head group, it is important to synthesize homologous series for systematic investigations of their physical and biological properties.

A number of recent studies [13–31] of a diverse variety of substituted carbohydrates have shown that the main molecular factors determining the type of thermotropic and lyotropic mesophases observed for liquid crystalline carbohydrate derivatives are the configuration of the hydrophilic (carbohydrate) part of the molecule, the number and length of the hydrophobic substituents, such as alkyl chains characteristic of liquid crystalline carbohydrate derivatives, and the degree and strength of hydrogen bonding with neighbouring molecules. However, the dependence of mesomorphic behaviour on the nature of the linkage between the hydrophilic and hydrophobic parts of liquid crystalline carbohydrates has been studied to a much lesser extent, although it has been reported recently [14] that some thioether and ester derivatives of D,L-xylitol, which is an open chain polyol, exhibit higher clearing points than those sugars with oxygen in place of the sulphur atom

*Author for correspondence; e-mail: S.M.Kelly@chem.hull.ac.uk
‡EPSRC Advanced Fellow.

or carboxy group. Many homologues of these xylitol derivatives were found to be soluble in water and were also reported to exhibit interesting lyotropic behaviour. Most thermal data for liquid crystalline carbohydrate derivatives to be found in the literature are for glucose, perhaps due to its ready availability and cheapness. However, recent investigations of the physical properties of other carbohydrates, such as galactose [24–27] in the pure state, as well as components of aqueous suspensions and emulsions with lyotropic liquid crystalline properties [28], indicate that they may exhibit a more advantageous property spectrum as biodegradable and biocompatible surfactants for non-denaturized proteins as well as detergents, compared with that of analogous glucose derivatives. It has also been reported that substituted sugars in the pyranose form with axial hydroxy groups, such as galactose, exhibit higher clearing points than those sugars, such as glucose, with only equatorial hydroxy groups with the same substituents, such as alkyl chains [24–27]. Therefore, we report here the synthesis of three short homologous series of related 6-*Z*-*n*-alkyl-α-D-galactopyranoses, namely 6-*O*-*n*-acyl-α-D-galactopyranoses ($Z = OCO$), 6-*S*-*n*-alkyl-6-thio-α-D-galactopyranoses ($Z = S$) and 6-*O*-(propylene-[3′-*S*-*n*-alkyl])-α-D-galactopyranoses ($Z = OC_3H_6S$). The nature of the linkage between the lipophilic and hydrophilic parts of the molecule has been varied in order to determine the effect of the nature of this linkage on the macroscopic liquid crystalline properties of these carbohydrates.

2. Synthesis

The 6-*Z*-*n*-alkyl derivatives of D-galactose (**5**; $Z = OCO$, S and OC_3H_6S), i.e. 6-*O*-*n*-acyl-α-D-galactopyranoses ($Z = OCO$; $n = 7$–11,13,15,17), 6-*S*-*n*-alkyl-6-thio-α-D-galactopyranoses ($Z = S$; $n = 8,10,12,14,16,18$) and 6-*O*-(propylene-[3′-*S*-*n*-alkyl])-α-D-galactopyranoses ($Z = OC_3H_6S$; $n = 8,10,12,14,16,18$), were prepared following the general synthetic pathways depicted in the scheme. The synthesis of 6-*O*-*n*-alkyl-α-D-galactopyranoses ($Z = O$; $n = 8,10,12,14,16,18$) has been reported previously [27]. The compounds (**5**) were prepared starting from 1,2:3,4-di-*O*-isopropylidene-α-D-galactopyranose (**1**), which was synthesized by the method of Régnault [32]. The esters (**5**; $Z = OCO$; $n = 7$–11,13,15,17) were obtained by reaction of the diacetal (**1**) with various acid chlorides in the presence of triethylamine to yield the protected intermediates (**4**; $Z = OCO$; $n = 7$–11,13,15,17). The deacetalization conditions with trifluoroacetic acid were

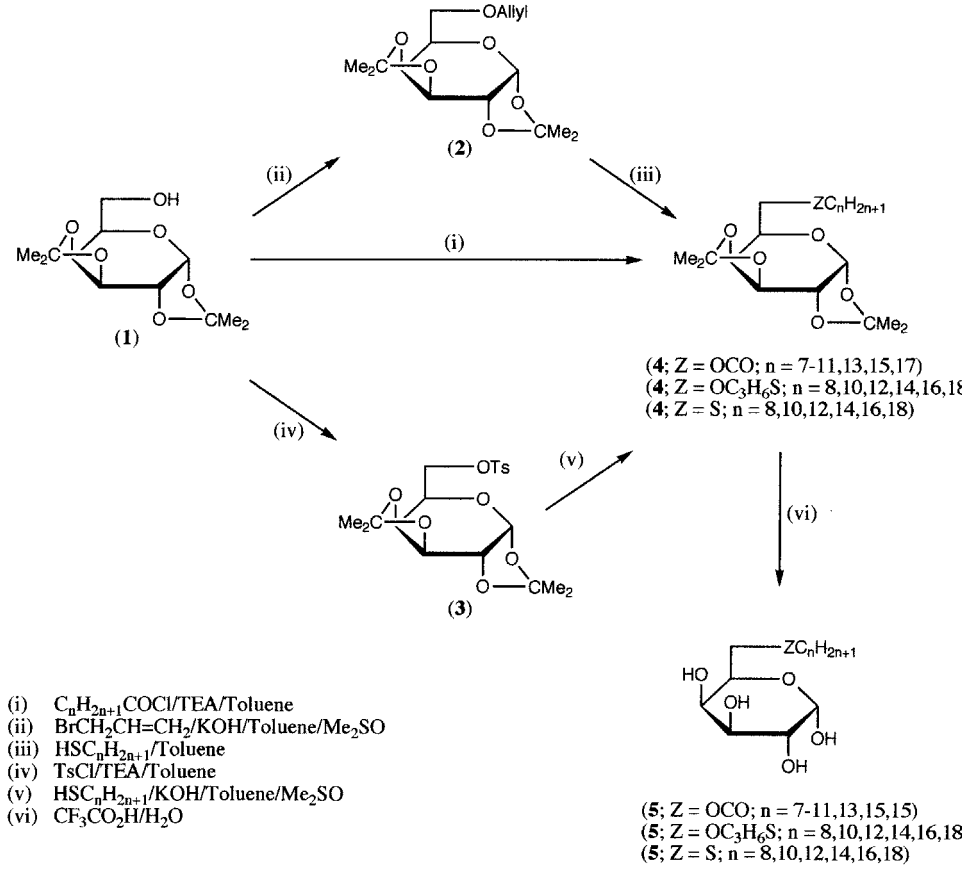

Scheme.

chosen to produce the α-configuration for the 6-*O*-*n*-acyl-α-D-galactopyranoses (**5**; $Z = OCO$; $n = 7–11,13,15,17$). The thioethers (**5**; $Z = S$; $n = 8,10,12,14,16,18$) were synthesized by tosylation of the diacetal substrate (**1**) to yield the protected tosylate (**3**) followed by reaction with HSC_nH_{2n+1} in the presence of potassium hydroxide to give the protected diacetals (**4**; $Z = S$; $n = 7–11,13,15,17$). Deacetalization with CF_3CO_2H gave the 6-*S*-*n*-alkyl-6-thio-α-D-galactopyranoses (**5**; $Z = S$; $n = 8,10,12,14,16,18$) in the α-configuration as above. The protected thioethers (**4**; $Z = OC_3H_6S$; $n = 8,10,12,14,16,18$) were obtained by reaction of the allylic intermediate (**2**), prepared by base-catalysed alkylation of (**1**) with allyl bromide, with various thiols in toluene at 80°C. Deacetalization with CF_3CO_2H gave the 6-*O*-(propylene-[3′-*S*-*n*-alkyl])-α-D-galactopyranoses (**5**; $Z = OC_3H_6S$; $n = 8,12,16,18$) as above.

3. Phase characterization

3.1. *Phase characterization by thermal optical microscopy*

The thermotropic mesophases observed for the four series of 6-*Z*-*n*-alkyl-α-D-galactopyranoses (**5**; $Z = OCO$, S, OC_3H_6S and O) studied exhibited almost identical textures during optical microscopy. All of the carbohydrates prepared exhibited the same enantiotropic mesophase on heating: the crystals melt on heating at a discrete temperature (T_m) to form a birefringent, fluid texture, see figure 1, which changed into an oily streak appearance of webbed focal conic-like defects at higher temperatures, see figure 2. This optical behaviour is typical of the SmA* phase, which is nearly always observed for liquid crystalline carbohydrates. At a higher temperature the preparation became optically extinct at the clearing point (T_{SmA^*-I}). Thermal decomposition was observed at or just above the clearing point for all of the homologues prepared. However, the focal conic texture was always formed on cooling, see figure 3, along with optically extinct homeotropic areas. The clearing point decreased on subsequent heating and cooling cycles. Nevertheless, fresh samples always gave the same melting and clearing point on the first heating cycle. The values for the clearing point were found to agree well (≈ 2–3°C) with those values determined by differential scanning calorimetry for nearly all of the homologues prepared, see §3.2. However, there was sometimes poor agreement (< 10°C) for the melting point for 6-*S*-*n*-alkyl-6-thio-α-D-galactopyranoses (**5**; $Z = S$) due to substantial thermal decomposition giving rise to very broad transitions during both types of measurement. Therefore, the values

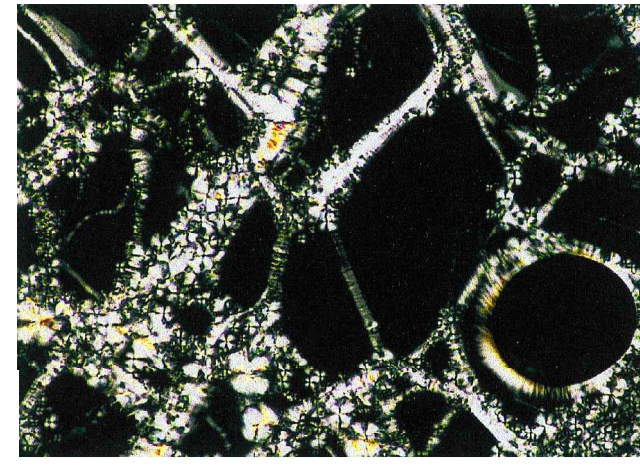

Figure 2. The oily streak texture with isotropic areas of decomposed material at 154°C just below the clearing point of 6-*O*-(propylene-[3′-*S*-octyl])-α-D-galactopyranose (**5**; $Z = OC_3H_6S$; $n = 8$) on a glass substrate (× 160).

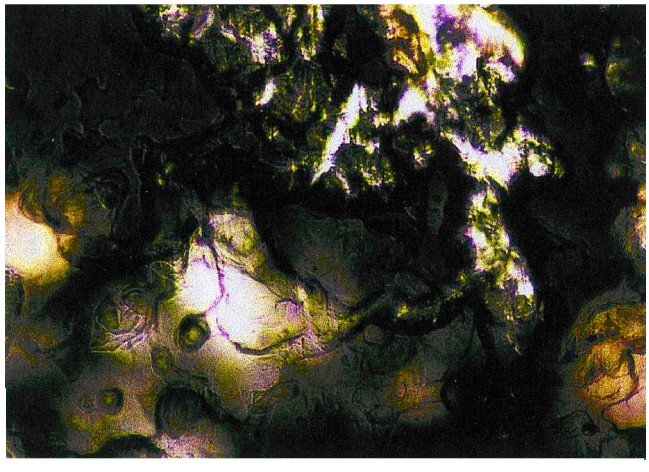

Figure 1. The texture observed on melting 6-*O*-(propylene-[3′-*S*-octyl])-α-D-galactopyranose (**5**; $Z = OC_3H_6S$; $n = 8$) at 95°C on a glass substrate (× 160).

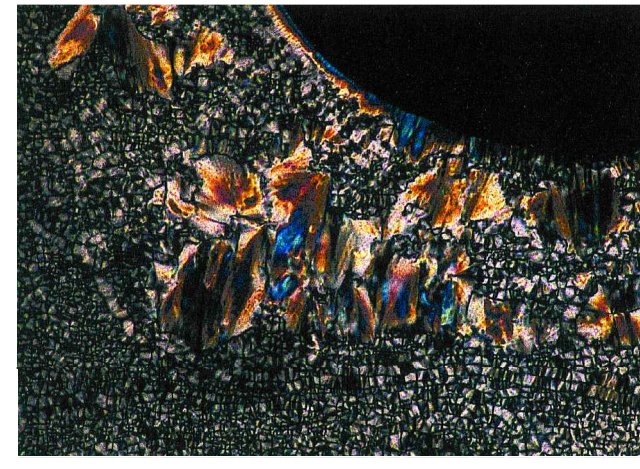

Figure 3. The focal conic defect texture of 6-*O*-(propylene-[3′-*S*-octyl])-α-D-galactopyranose (**5**; $Z = OC_3H_6S$; $n = 8$) formed on cooling from the isotropic liquid down to 150°C on a glass substrate (× 160).

for the melting point listed in table 1 for this series of carbohydrates are those obtained from microscopy and reflect the temperature at which the compound was judged to have melted. Therefore, a degree of subjectivity in these measurements cannot be excluded. These broad melting transitions are most probably attributable to the sulphur atom, as the corresponding 6-*O*-*n*-alkyl-α-D-galactopyranoses (**5**; $Z = O$) [27] are much more stable and good agreement between T_m values obtained from DSC measurements and microscopy was found, see above. Upon cooling from the isotropic liquid, bâtonnets were observed, which coalesced spontaneously in the bulk to form focal conic domains, see figure 3. As the sample is cooled further, the polar hydrophilic end of the carbohydrate molecules sometimes tended to adhere more strongly to the glass surface via hydrogen bonding. Thus, most of the resultant texture becomes homeotropic and optically extinct between crossed polarizers, which indicates that the phase is optically uniaxial. However, focal conic defects could still be observed in parts of the area of view and especially around air bubbles and at the edges of the preparation for all of the materials prepared. This optical behaviour, i.e. simultaneous presence of both homeotropic and focal conic textures, indicates that the mesophase observed is a calamitic smectic A* phase (SmA*). The elliptical and hyperbolic lines of optical discontinuity characteristic of focal conic defects were also observed, which classifies the mesophase as being smectic A* with a layered structure, where the long axes of the molecules are on average orthogonal to the layer planes and the in-plane and out-of-plane positional ordering of the molecules is short range, see §3.3.

Table 1. Transition temperatures (°C) and some enthalpies ($J\,g^{-1}$) of transition for the 6-*Z*-*n*-alkyl-α-D-galactopyranoses (**5**).

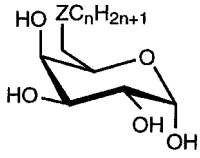

n	Cr	SmA*	I
		$Z = OCO$	
7	•	85 (8.1) •	133 (2.0) •
8	•	90 (101.9) •	155 (1.9) •
9	•	87 (85.5) •	175 (2.3) •
10	•	115 (74.0) •	181 (8.6) •
11	•	94 (63.9) •	182 (11.1) •
13	•	117 (70.3) •	184 (2.2) •
15	•	118 (104.6) •	182 (1.6) •
17	•	114 (74.7) •	181 (1.8) •
		$Z = S$	
8	•	98 •	173 •
10	•	104 (90.5) •	191 (11.4) •
12	•	109 (120.9) •	185 (7.8) •
14	•	100 (105.1) •	183 (7.5) •
16	•	103 (140.0) •	181 (8.2) •
18	•	114 (152.6) •	177 (3.3) •
		$Z = OC_3H_6S$	
8	•	95 (128.5) •	156 (3.9) •
10	•	101 (137.6) •	166 (1.4) •
12	•	99 (139.8) •	165 (1.9) •
14	•	109 (148.0) •	163 (1.5) •
16	•	90 (111.2) •	162 (1.1) •
18	•	104 (139.2) •	154 (0.8) •
		$Z = O$	
8	•	113 (117.1) •	169 (7.75) •
10	•	117 (72.7) •	172 (1.87) •
12	•	119 (127.8) •	171 (3.70) •
14	•	114 (118.1) •	169 (6.92) •
16	•	121 (127.1) •	167 (1.58) •
18	•	119 (125.6) •	164 (1.16) •

3.2. *Phase characterization by differential scanning calorimetry*

The enthalpy values for the melting (T_m) and clearing points ($T_{Sm\,A^*\text{-}I}$) of the 6-*O*-*n*-acyl-α-D-galactopyranoses (**5**; $Z = OCO$), 6-*S*-*n*-alkyl-6-thio-α-D-galactopyranoses (**5**; $Z = S$) and 6-*O*-(propylene-[3′-*S*-*n*-alkyl])-α-D-galactopyranoses (**5**; $Z = OC_3H_6S$) prepared in this work and the 6-*O*-*n*-alkyl-α-D-galactopyranoses (**5**; $Z = O$) reported previously [27] are collated in brackets in table 1. It is clear that the transitions T_m and $T_{Sm\,A^*\text{-}I}$ are both first order transitions. The clearing point enthalpies are relatively small in comparison to the melting enthalpies. The values measured are of a similar magnitude to those found in conventional liquid crystal systems which exhibit SmA* to isotropic liquid transitions, although the variations are quite large (0.8–11.4 $J\,g^{-1}$) for $T_{Sm\,A^*\text{-}I}$ and much larger than the percentage change for T_m (63.9–148.0 $J\,g^{-1}$). These values were determined twice on heating and cooling cycles on the same sample. The value found on the first heating cycle is quoted in the table. The other values varied considerably due to thermal decomposition. However, the values obtained on separate samples of the same compounds were generally reproducible, although variations were found for some homologues due to the onset of thermal degradation at or just above $T_{Sm\,A^*\text{-}I}$. This renders an interpretation of these large variations in the enthalpy of the SmA* to isotropic liquid transition of dubious value. As the solubility of an amphiphile in water is mainly determined [33] by the amount of energy required to overcome the crystal lattice forces, the high values sometimes found for the melting process of the same homologues indicate that these materials will be sparingly soluble in water and indeed this was found to be the case. The large enthalpy values determined for T_m compared with those found for $T_{Sm\,A^*}$ indicate that these values correspond

to the breaking of a three-dimensional crystal lattice primarily held together by intermolecular hydrogen bonding between the carbohydrate moieties, which defines the melting point [30]. This is followed by the breaking down at the clearing point of the less ordered and fluid bilayer structure of the SmA* phase, stabilized by van der Waals forces between the aliphatic chains, to give the isotropic liquid. Some residual hydrogen bonding will no doubt still be present in the liquid crystalline and liquid states. The low T_m enthalpy values found for the 6-*O*-(propylene-[3′-*S*-*n*-alkyl])-α-D-galactopyranoses (**5**; $Z = OC_3H_6S$) compared with those of the other three series of carbohydrates may be due either to the presence of the heteroatom in the terminal chain or to the somewhat lower purity of this particular series.

Typical heating thermograms for one homologue with approximately the same chain length of each of the four series, i.e. 6-*O*-tetradecanoyl-α-D-galactopyranose (**5**; $Z = OCO$; $n = 13$), 6-*S*-tetradecyl-6-thio-α-D-galactopyranose (**5**; $Z = S$; $n = 14$), 6-*O*-(propylene-[3′-*S*-decyl])-α-D-galactopyranose (**5**; $Z = OC_3H_6S$; $n = 10$) and 6-*O*-tetradecyl-α-D-galactopyranose (**5**; $Z = O$; $n = 14$) [27], are shown in figures 4–7, respectively. The heating thermograms for 6-*O*-*n*-acyl-α-D-galactopyranoses (**5**; $Z = OCO$) and 6-*S*-*n*-alkyl-6-thio-α-D-galactopyranoses (**5**; $Z = S$) often exhibit a steep slope for the base line, very broad peaks and clear thermal decomposition at or just above $T_{Sm A^*-I}$, see figures 4 and 5. Agreement between the values for the melting and clearing point obtained by DSC and optical microscopy is good for the 6-*O*-*n*-acyl-α-D-galactopyranoses (**5**; $Z = OCO$) and poor for the 6-*S*-*n*-alkyl-6-thio-α-D-galactopyranoses (**5**; $Z = S$). There are often differences of 20°C between the onset temperature and the peak temperature of a transition for the latter, see figure 5. This is due to substantial thermal decomposition on heating during both types of measurements. The 6-*O*-(propylene-[3′-*S*-*n*-alkyl])-α-D-galactopyranoses (**5**; $Z = OC_3H_6S$) prepared in this work and the 6-*O*-*n*-alkyl-α-D-galactopyranoses (**5**; $Z = O$) reported previously [27] appear to be much more stable to heat. The base lines are relatively flat and sharp transition peaks are observed, see figures 6 and 7.

3.3. *X-ray analysis*

The experimental values for the *d*-spacings found for 6-*S*-decyl-6-thio-α-D-galactopyranose (**5**; $Z = S$; $n = 10$) measured at a scan rate of 2°C min^{-1}, see §5, are plotted against temperature in figure 8. Phase reflections relating to a layer spacing of 33.7 Å ($d_1 = 32.2$ and $d_2 = 16.0$ Å) were observed at 103°C in the fully formed SmA* phase above T_m. The layer spacing decreases with increasing temperature. This is accompanied by a marked decrease of the scattering intensity associated with d_2. Similar behaviour has been found for other carbohydrate materials [27]. It can be attributed to a decrease in order within the phase at higher temperature. Above 160°C the d_2 reflection disappears altogether, which is indicative of an almost complete loss of order in the smectic phase. Above 184°C, where a layer spacing of 28.7 Å was found, the transition to the isotropic liquid had already occurred

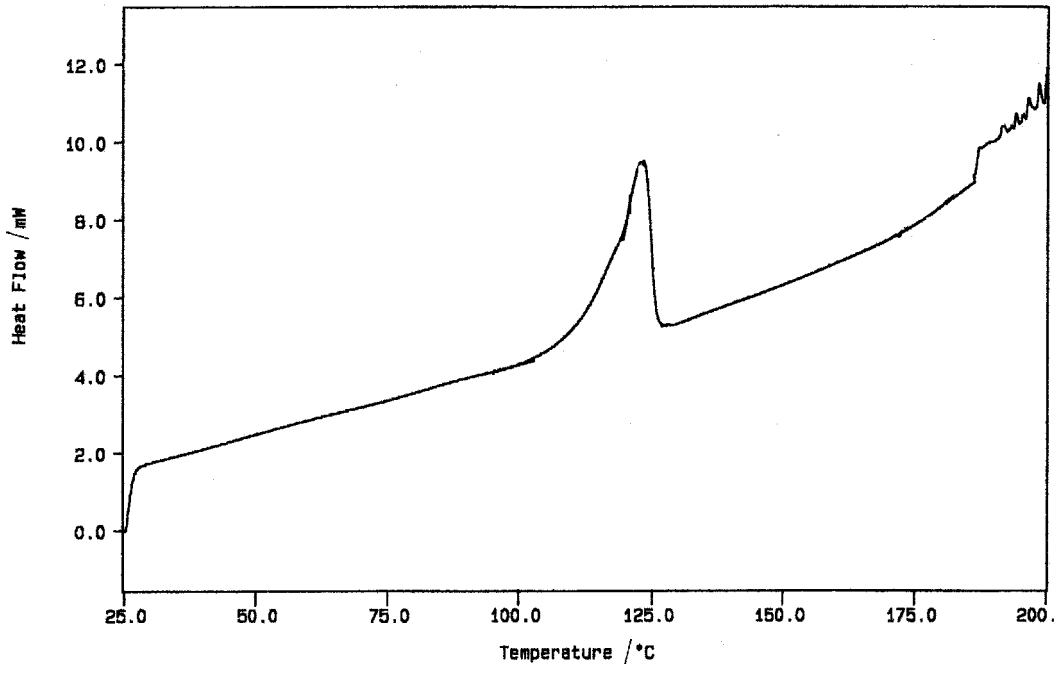

Figure 4. Differential scanning thermogram as a function of temperature for the first heating cycle for the 6-*O*-tetradecanoyl-α-D-galactopyranose (**5**; $Z = OCO$; $n = 13$), scan rate 10°C min^{-1}.

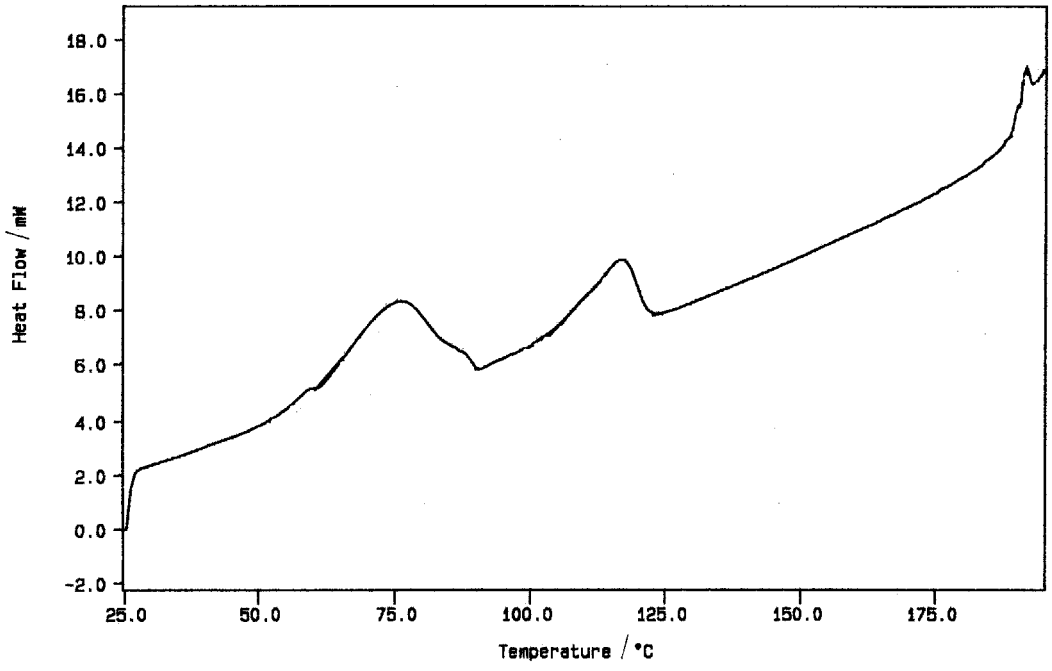

Figure 5. Differential scanning thermogram as a function of temperature for the first heating cycle for the 6-*S*-tetradecyl-6-thio-α-D-galactopyranose (**5**; $Z = S$; $n = 14$), scan rate 10°C min^{-1}.

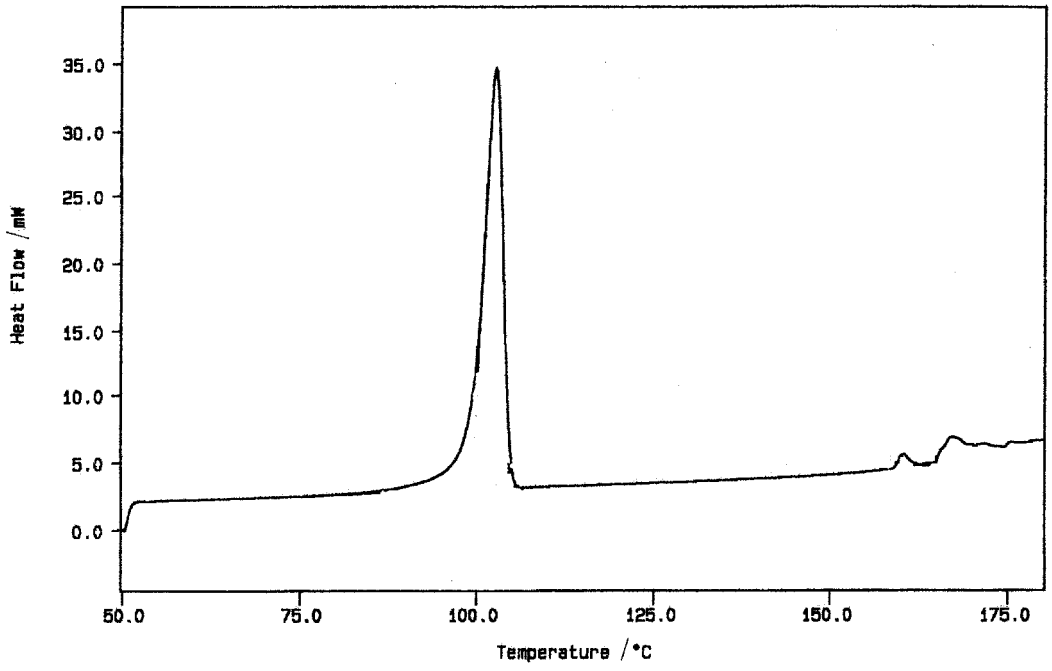

Figure 6. Differential scanning thermogram as a function of temperature for the first heating cycle for the 6-*O*-(propylene-[3′-*S*-decyl])-α-D-galactopyranose (**5**; $Z = OC_3H_6S$; $n = 10$), scan rate 10°C min^{-1}.

due to thermal decomposition ($T_{Sm A^*-I} = 191$°C according to optical microscopy). The estimation of the maximum molecular length for 6-*S*-decyl-6-thio-α-D-galactopyranose (**5**; $Z = S$; $n = 10$) obtained from modelling the molecular structure, using the Cerius2 (3.5) software from MSI, yields a value of 17.2 Å [27]. A bipolar smectic A phase has a calculated layer spacing of 34.4 Å (2 × 17.2 Å). This corresponds reasonably well with the observed value of 32.2 Å for the layer spacing. Thus, 6-*S*-decyl-6-thio-α-D-galactopyranose (**5**; $Z = S$; $n = 10$) appears to form a SmA* phase with a bilayer structure without any interdigitation of the molecular core or the terminal chain.

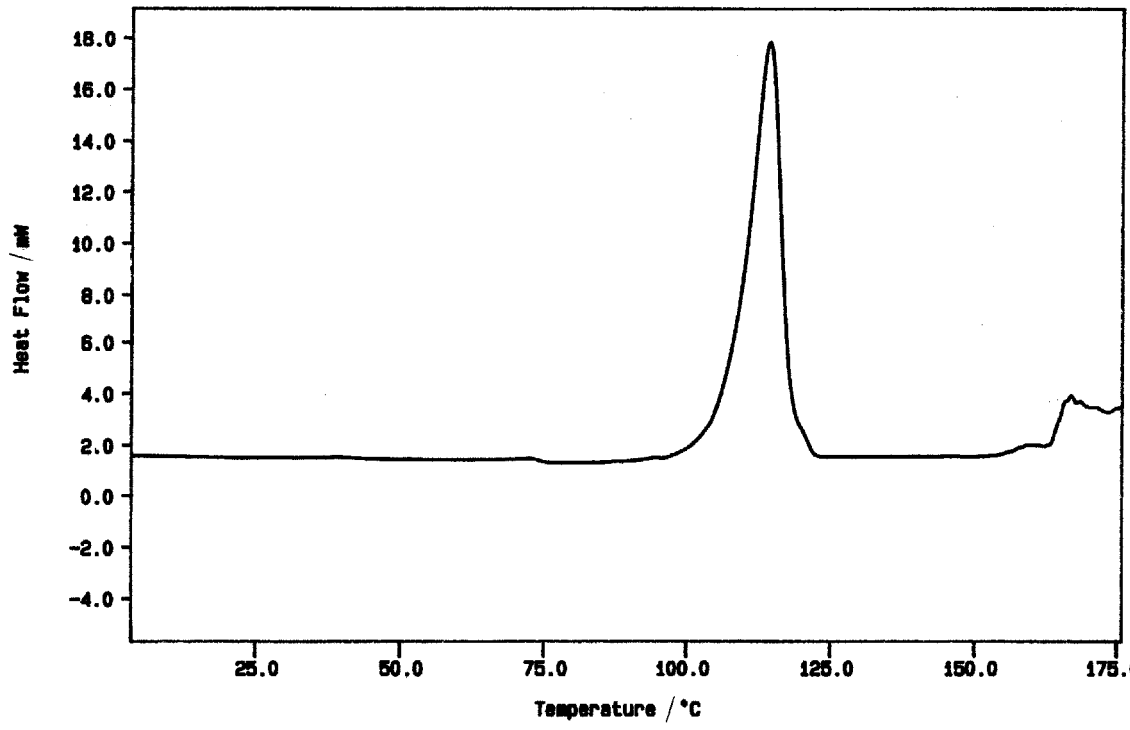

Figure 7. Differential scanning thermogram as a function of temperature for the first heating cycle for the 6-*O*-tetradecyl-α-D-galactopyranose (**5**; $Z = O$; $n = 14$) [27], scan rate 10°C min^{-1}.

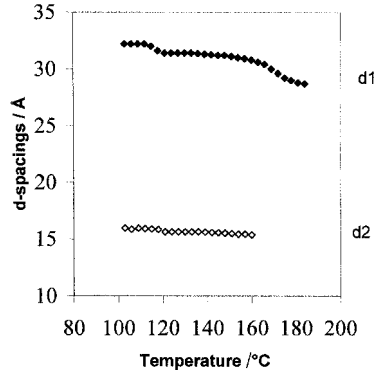

Figure 8. The experimental values for the *d*-spacings for 6-*S*-decyl-6-thio-α-D-galactopyranose (**5**; $Z = OC_3H_6S$; $n = 10$), scan rate 2°C min^{-1}.

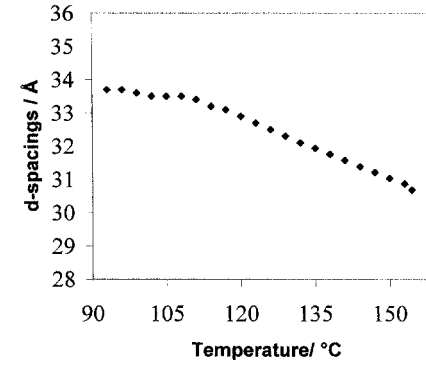

Figure 9. The experimental values for the *d*-spacings for 6-*O*-(propylene-[3′-*S*-octyl])-α-D-galactopyranose (**5**; $Z = OC_3H_6S$; $n = 8$), scan rate 2°C min^{-1}.

The experimental values for the *d*-spacings measured at a scan rate of 3°C min^{-1} for 6-*O*-(propylene-[3′-*S*-octyl])-α-D-galactopyranose (**5**; $Z = OC_3H_6S$; $n = 8$) are plotted against temperature in figure 9. The melting to the liquid crystalline phase at 95°C, as identified by optical polarizing microscopy, could also be observed in the X-ray measurements. Reflections associated with a layer spacing of 33.7 Å were detected just above T_m. With increasing temperature, a continuous contraction of the layer spacing to 30.7 Å up to $T_{Sm A^*-I}$ at 156°C was observed. Above that temperature the transition to the isotropic liquid had clearly occurred. The calculated molecular length of 6-*O*-(propylene-[3′-*S*-octyl])-α-D-galactopyranose (**5**; $Z = OC_3H_6S$; $n = 8$) is 24.3 Å. Therefore, the calculated spacing for a bipolar SmA* phase would be about 48 Å. However, a layer spacing of only 33.7 Å is found. This implies that some degree of molecular interdigitation must be present in the bipolar SmA* phase observed. Since the only major difference between 6-*S*-decyl-6-thio-α-D-galactopyranose (**5**; $Z = S$) and 6-*O*-(propylene-[3′-*S*-octyl])-α-D-galactopyranose (**5**; $Z = OC_3H_6S$; $n = 8$) is the presence of the sulphur

atom in the chain and a slightly longer chain length and as no interdigitation of the cores is found for 6-*S*-decyl-6-thio-α-D-galactopyranose (**5**; $Z = S$), it can be assumed that interdigitation of the terminal chain of the molecules takes place for 6-*O*-(propylene-[3′-*S*-decyl])-α-D-galactopyranose (**5**; $Z = OC_3H_6S$; $n = 8$). The value of 33.7 Å observed upon melting to form the SmA* phase corresponds approximately to interdigitation of the alkyl chains up to the sulphur atoms in the chain, which would give a layer spacing of about 35.5 Å. Thus, it is concluded that 6-*O*-(propylene-[3′-*S*-octyl])-α-D-galactopyranose (**5**; $Z = OC_3H_6S$; $n = 8$) exhibits an interdigitated bipolar SmA* between the melting and clearing points.

Thus, the conclusion to be drawn from the X-ray diffraction experiments is that the introduction of an additional propyloxy spacer group into 6-*S*-*n*-alkyl-6-thio-α-D-galactopyranoses (**5**; $Z = S$) to form the 6-*O*-(propylene-[3′-*S*-*n*-alkyl])-α-D-galactopyranoses (**5**; $Z = OC_3H_6S$) leads to a variation of the phase structure. The presence of the additional propyloxy spacer group results in a difference in the degree of interdigitation of the terminal alkyl chains of the 6-*O*-(propylene-[3′-*S*-*n*-alkyl])-α-D-galactopyranoses (**5**; $Z = OC_3H_6S$) compared with that of the 6-*S*-*n*-alkyl-6-thio-α-D-galactopyranoses (**5**; $Z = S$).

4. Discussion of the transition temperatures

The liquid crystal transition temperatures of the 6-*O*-*n*-acyl-α-D-galactopyranoses (**5**; $Z = OCO$; $n = 7$–11,13,15,17) are collated in table 1 and plotted against the number (n) of methylene units in the terminal chain in figure 10. $T_{Sm A^*\text{-}I}$ increases from low values for short alkyl chains, but then reaches a maximum before decreasing gradually as the chain becomes longer. T_m shows a certain degree of alternation and a general tendency to increase with increasing chain length, although the differences for the absolute values of T_m are generally small. Therefore, a broad SmA* phase is observed for most homologues of the 6-*O*-*n*-acyl-α-D-galactopyranoses (**5**; $Z = OCO$; $n = 7$–11,13,15,17) after a critical length of the alkyl chain ($n = 5$) has been attained, although most homologues exhibit high T_m and $T_{Sm A^*\text{-}I}$.

The 6-*S*-*n*-alkyl-6-thio-α-D-galactopyranoses (**5**; $Z = S$; $n = 8,10,12,14,16,18$) exhibit high T_m and $T_{Sm A^*\text{-}I}$, see table 1 and figure 11. Therefore a broad SmA* phase is observed for most homologues. T_m is almost independent of chain length, whereas $T_{Sm A^*\text{-}I}$ increases from low values for short alkyl chain lengths, reaches a maximum and then decreases gradually as the chain becomes longer. The 6-*S*-*n*-alkyl-6-thio-α-D-galactopyranoses (**5**; $Z = S$; $n = 8,10,12,14,16,18$) possess clearing points at higher temperatures and melting points at lower temperatures than those of the corresponding 6-*O*-*n*-alkyl-α-D-galactopyranoses, see figure 11, but lower than those of the corresponding homologues of the 6-*O*-*n*-acyl-α-D-galactopyranoses. This is probably attributable to a higher degree of molecular polarizability of the esters and thioethers, although the effect could well have been expected to be much smaller than that observed considering the strong intermolecular hydrogen bonding between the four hydroxyl groups on adjacent carbohydrates molecules.

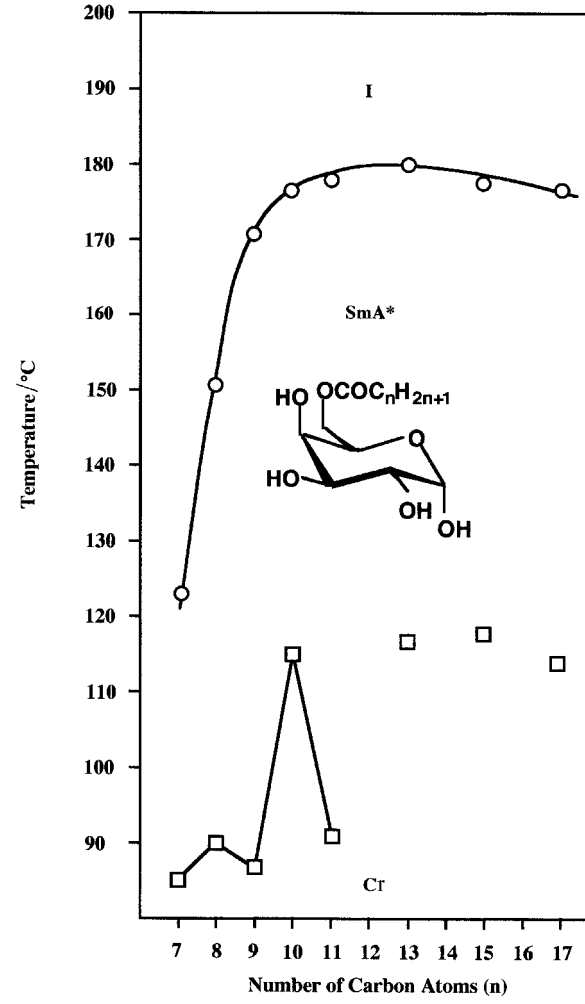

Figure 10. Plot of the transition temperatures of the 6-*O*-*n*-acyl-α-D-galactopyranoses (**5**; $Z = OCO$; $n = 7$–11,13,15,17) against the number of the carbon atoms (n) in the alkyl part of the alkyl terminal chain

The liquid crystal transition temperatures of the 6-*O*-(propylene-[3′-*S*-*n*-alkyl])-α-D-galactopyranoses (**5**; $Z = OC_3H_6S$; $n = 8,12,16,18$) also recorded in table 1 are significantly lower than those of the corresponding esters, ethers or thioethers (**5**; $Z = OCO$, O, S). This may be due to intermolecular dipole–dipole interactions attributable to non-conjugated heteroatoms, although this may be caused by the lower length/breadth ratio of molecular dimers as revealed by X-ray analysis. This is

shown more clearly by the thermal data in table 2 where it can be seen that the replacement of a methylene group in the middle of a chain of the 6-*O*-dodecyl-α-D-galactopyranose (**5**; $Z = O$; $n = 12$) by a sulphur atom to produce the 6-*O*-(propylene-[3′-*S*-*n*-octyl])-α-D-galactopyranose (**5**; $Z = OC_3H_6S$; $n = 8$) leads to a lower clearing point for the latter. This may have parallels with similar behaviour found for non-amphiphilic liquid crystals and is not well understood [34].

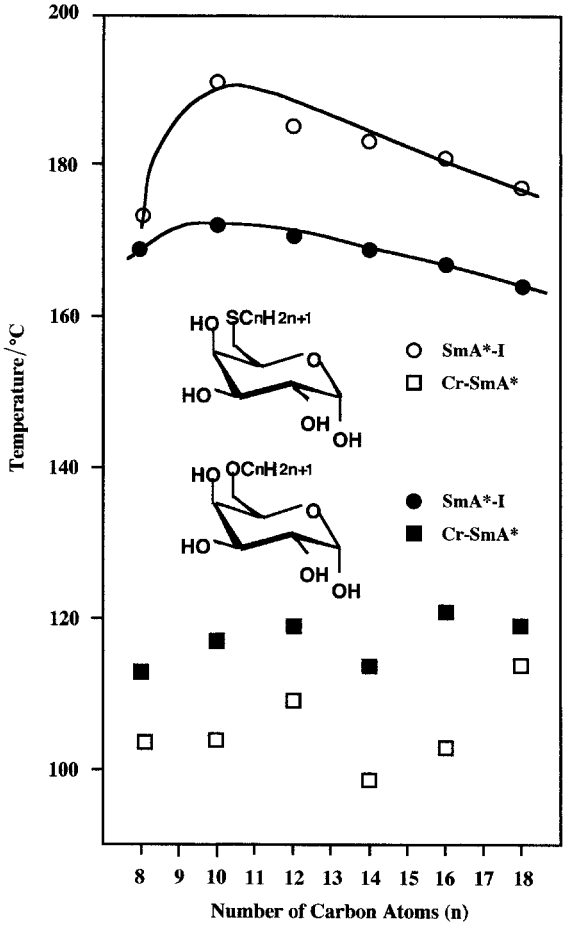

Figure 11. Plot of the transition temperatures of the 6-*S*-*n*-alkyl-6-thio-α-D-galactopyranoses (**5**; $Z = S$; $n = 8,10,12,14,16,18$) and the 6-*O*-*n*-alkyl-α-D-galactopyranoses (**5**; $Z = O$; $n = 8,10,12,14,16,18$) against the number of the carbon atoms (n) in the alkyl part of the alkyl terminal chain.

Table 2. Transition temperatures (°) for the 6-*O*-(propylene-[3′-*S*-octyl])-α-D-galactopyranose (**5**; $Z = OC_3H_6S$; $n = 8$) and the 6-*O*-dodecyl-α-D-galactopyranose (**5**; $Z = O$; $n = 12$) [27].

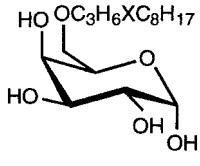

Compound	X	Cr		SmA*		I
($Z = OC_3H_6S$; $n = 8$)	S	•	95	•	156	•
($Z = O$; $n = 12$)	CH_2	•	119	•	171	•

Therefore, the order of efficiency of the linking group Z in favouring liquid crystal formation for the same homologues of the 6-*O*-*n*-acyl-α-D-galactopyranoses ($Z = OCO$), 6-*S*-*n*-alkyl-6-thio-α-D-galactopyranoses ($Z = S$), 6-*O*-*n*-alkyl-α-D-galactopyranoses ($Z = O$) and 6-*O*-(propylene-[3′-*S*-*n*-alkyl])-α-D-galactopyranoses (OC_3H_6S), based on comparisons of the clearing point, is:

$$S \approx OCO > O > OC_3H_6S$$

The 6-*O*-(propylene-[3′-*S*-*n*-alkyl])-α-D-galactopyranoses (OC_3H_6S) exhibit a broader mesophase range than the corresponding 6-*O*-*n*-alkyl-α-D-galactopyranoses ($Z = O$), due to lower melting points for each homologue of the former, but otherwise the order is the same based on mesophase range. This correlates well with the order of polarizability of the linking unit Z for the first three members of the series (except for the 6-*O*-(propylene-[3′-*S*-*n*-alkyl])-α-D-galactopyranoses, where the presence of a sulphur atom in the middle of a chain gives rise to a lower clearing point) and is in good agreement with the mesomorphic behaviour of related homologous series of ester, ether and thioether derivatives of D,L-xylitol [14].

5. Experimental

5.1. *Characterization*

NMR spectra were recorded using a Bruker WB-300 and the solvents $CDCl_3$, $(CD_3)_2SO$ or C_5D_5N (internal Me_4Si). Reactions were monitored by either HPLC (Waters 721), using one of the reverse phase columns RP-18 (Merck) or PN 27-196 (Waters) or CPG (Girdel) with columns of either OV 17 or SE 30. The structures of all the compounds were determined by ^1H and ^{13}C NMR spectroscopy.

The purity of the compounds was determined by thin layer chromatography (TLC), high performance liquid chromatography (HPLC), elemental analysis (CHS) and differential scanning calorimetry (DSC); 4 × 8 cm precoated TLC plates, SiO_2 SIL G/UV_{254}, layer thickness 0.25 mm (Machery-Nagel, Düren, Germany) were utilized. The purity of the 6-*O*-*n*-acyl-α-D-galactopyranoses (**5**; $Z = OCO$; $n = 7$–$11,13,15,17$) and the 6-*S*-*n*-alkyl-6-thio-α-D-galactopyranoses (**5**; $Z = S$; $n = 8,10,12,14,16,18$) as determined by elemental analysis was satisfactory (> 99.5%) for all the homologues prepared and very good (> 99.9%) for most homologues. Despite repeated recrystallization, the purity of the 6-*O*-(propylene-[3′-*S*-*n*-alkyl])-α-D-galactopyranoses (**5**; $Z = OC_3H_6S$;

$n = 8,10,12,14,16,18$) was unsatisfactory for some homologues (> 98.0%), although DSC indicated a higher purity (> 99.5%) and optical microscopy also revealed a relatively sharp clearing point for the carbohydrate derivatives. Melting points were determined with a Büchi apparatus and are uncorrected. Optical rotations were recorded at room temperature in $CHCl_3$ solutions with a Perkin-Elmer 241 polarimeter using a 1 dm cell.

Column chromatography was performed on silica gel (60 mesh, Matrex) by gradient elution with hexane–acetone (in each case the ratio of silica gel to product mixture to be purified was 30 : 1). Reaction solvents and liquid reagents were purified by distillation or drying shortly before use. Reactions were carried out under nitrogen unless water was present as a reagent or a solvent. All temperatures were measured externally unless otherwise stated.

Mesophase identification and the determination of the transition temperatures of the carbohydrates prepared were determined by optical microscopy using either a Zeiss Universal or an Olympus BH-2 polarizing light microscope in conjunction with a Mettler FP 52 microfurnace and FP 5 Central Processor.

DSC was used to determine the enthalpies of transition and to confirm the phase transition temperatures determined by optical microscopy. Thermograms (scan rate 10°C min^{-1}) were obtained using a Perkin Elmer DSC 7 operating on 7 series/UNIX software. The results obtained were standardized with respect to indium (measured onset 156.68°C, ΔH 28.47 J g^{-1}, literature value 156.60°C, ΔH 28.45 J g^{-1}), nitrotoluene (measured onset 51.17°C, ΔH 118.49 J g^{-1}, literature value 51.63°C, ΔH 122.58 J g^{-1}) and benzil (measured onset 94.42°C, ΔH 108.52 J g^{-1}, literature value 94.87°C, ΔH 92.68 J g^{-1}).

Comparison of the transition temperatures determined by optical microscopy and DSC show some discrepancies of about 2–3°C. These differences can be attributed to decomposition at elevated temperatures at a rate which depends on the rate of heating, the time spent at an elevated temperature and the nature of the supporting substrate, e.g. the materials decomposed more quickly in aluminium DSC pans than in gold DSC pans, or on glass microscope slides.

In order to characterize the solid state of these materials, 6-*S*-*n*-decyl-6-thio-α-D-galactopyranose (**5**; $Z = S$; $n = 10$) and the 6-*O*-(propylene-[3′-*S*-*n*-octyl])-α-D-galactopyranose (**5**; $Z = OC_3H_6S$; $n = 8$) were investigated using X-ray diffraction. The tendency of carbohydrates to decompose at high temperatures required an experimental set-up allowing for the recording of sufficient data before degradation of the sample set in. Thus high flux synchrotron radiation was employed, using the experimental set-up of station 8.2 at Daresbury Laboratories, described elsewhere [35–38]. Samples were prepared as polycrystalline powders in Lindemann tubes and maintained at a controlled temperature allowing for the recording of diffraction data whilst performing a temperature scan of 2 or 3°C min^{-1} in the temperature range of 90 to 200°C. The selected experimental set-up was limited to the recording of data relating to lattice parameters greater than 17.8 Å. The use of wet rat-tail collagen as calibration standard leads to a systematic error of 3% of the observed *d*-spacings [38].

5.2. *General synthetic procedures*

5.2.1. *6-O-Alkyl-1,2 : 3,4-di-O-isopropylidene-α-D-galactopyranose (**2**)*

Finely powdered potassium hydroxide (2.4 equiv.) and allyl bromide (1.2 equiv.) were added to a stirred solution of the 1,2 : 3,4-di-*O*-isopropylidene-α-D-galactopyranose (**1**) (1 equiv.) in 4 : 1 toluene : dimethyl sulphoxide (100 g l^{-1}) at room temperature. After complete reaction (2 h), the mixture was filtered and the filtrate neutralized with saturated aqueous ammonium chloride. The organic phase was separated, washed with water (twice), dried (Na_2SO_4) and the solvent removed under reduced pressure. Purification by column chromatography (solvent mixture hexane : acetone 24 : 1 v/v) yielded 6-*O*-alkyl-1,2 : 3,4-di-*O*-isopropylidene-α-D-galactopyranose (**2**) as an oil (96%); $[\alpha]_D^{27} = -68.3$ ($c = 1$; $CHCl_3$).

5.2.2. *6-O-p-Toluenesulphonyl-1,2 : 3,4-di-O-isopropylidene-α-D-galactopyranose (**3**)*

p-Toluenesulphonyl chloride (1 equiv.) and triethylamine (1.1 equiv.) were added at room temperature to a mixture of the 1,2 : 3,4-di-*O*-isopropylidene-α-D-galactopyranose (**1**) in toluene (100 g l^{-1}). After 24 h the mixture was filtered and the solvent removed under reduced pressure. The crude product was recrystallized from a mixture of 5 : 1 hexane–acetone giving the pure tosylate (**3**) in 92% yield; m.p. = 102.5–104.3°C; $[\alpha]_D^{22} = -68.7$ ($c = 1.5$; $CHCl_3$).

5.2.3. *6-O-n-Acyl-1,2 : 3,4-di-O-isopropylidene-α-D-galactopyranoses (**4**; Z = OCO; n = 7–11,13,15,17)*

Triethylamine (1.1 equiv.) was added to a stirred solution of the 1,2 : 3,4-di-*O*-isopropylidene-α-D-galactopyranose (**1**) in toluene (100 g l^{-1}) at room temperature, followed by the appropriate acid chloride (1 equiv.). After complete reaction (1 to 3 h), the mixture was filtered and the solvent removed under reduced pressure. The raw reaction products were purified by column chromatography (solvent mixture hexane : acetone 24 : 1 v/v) and recrystallization from tetrahydrofuran to give the desired products in 90 to 95% yields, except for the stearic ester (70%). All the acid chlorides used were commercially available except for decanoyl chloride which was prepared by the reaction of thionyl chloride

(1.2 equiv.) with the corresponding acid (1 equiv.) in toluene, in the presence of pyridine (1 equiv.) at 110°C. After 24 h, the solvent was removed under reduced pressure until the volume of the mixture was reduced by 50%. The resulting solution was then used to esterify the diacetal (**1**) as described above.

5.2.4. *6-O-(Propylene-(3′-S-n-Alkyl))-1,2:3,4-di-O-isopropylidene-α-D-galactopyranoses (**4**; Z = OC_3H_6S; n = 8,10,12,14,16,18)*

Thioetherification was achieved via the addition of the appropriate alkyl thiol (2 equiv.) at 80°C, to a stirred solution of 6-*O*-alkyl-1,2:3,4-di-*O*-isopropylidene-α-D-galactopyranose (**2**) (1 equiv.) in toluene (200 g l^{-1}). After 24 h, the solvent was removed under reduced pressure and the desired products were isolated after purification by column chromatography (hexane) in 80 to 90% yields.

5.2.5. *6-S-n-Alkyl-1,2:3,4-di-O-isopropylidene-α-D-galactopyranoses (**4**; Z = S; n = 8,10,12,14,16,18)*

Thioetherification was achieved via dropwise addition of a solution of the appropriate alkyl thiol (1.2 equiv.) in toluene, at 60°C, to a stirred solution of KOH (2.4 equiv.) and 6-*O*-*p*-toluenesulphonyl-1,2:3,4-di-*O*-isopropylidene-α-D-galactopyranose (**3**) (1 equiv.) in 4:1 toluene–dimethyl sulphoxide (100 g l^{-1}). After complete reaction (1 to 4 h), the mixture was filtered, and the filtrate neutralized with saturated aqueous ammonium chloride solution. The organic phase was separated, washed with water (twice), dried (Na_2SO_4), and the solvent removed under reduced pressure. The desired products were isolated after purification by column chromatography (solvent mixture hexane:acetone 49:1 v/v) in 88 to 95% yields.

5.2.6. *6-Z-n-alkyl-α-D-galactopyranoses (**5**; Z = OCO; n = 7–11,13,15,17; Z = OC_3H_6S; n = 8,10,12,14,16,18; Z = S; n = 8,10,12,14,16,18).*

The appropriate diacetal D-galactose derivative (**4**; Z = OCO; n = 7–11,13,15,17; Z = OC_3H_6S; n = 8,10,12.14,16,18; Z = S; n = 8,10,12,14,16,18) was added to a stirred solution of trifluoroacetic acid:water 9:1 (v/v) (500 g l^{-1}), at room temperature. After 15 min, cold diethyl ether was added and the solution cooled to – 20°C. The desired products were filtered off, washed with diethyl ether (twice) and recrystallized from diethyl

Table 3. Yields and physical constant data for the 6-*Z*-*n*-alkyl-α-D-galactopyranoses (**5**).

Compound *n*	Yields[a]/%	$[\alpha]_D^{23}$ [b]	MW	Formula	Calculated/% C	Calculated/% H	Found/% C	Found/% H
				Z = OCO				
7	46	56.2	306.35	$C_{14}H_{26}O_7$	54.88	8.55	55.15	8.69
8	64	55.9	320.38	$C_{15}H_{28}O_7$	56.23	8.81	56.64	9.06
9	66	45.0	334.41	$C_{16}H_{30}O_7$	57.46	9.04	57.82	9.32
10	71	42.1	348.43	$C_{17}H_{32}O_7$	58.60	9.25	59.46	9.58
11	74	41.9	362.46	$C_{18}H_{34}O_7$	59.64	9.45	59.93	9.58
13	92	39.4	390.51	$C_{20}H_{38}O_7$	61.51	9.80	61.72	9.97
15	89	32.5	418.57	$C_{22}H_{42}O_7$	63.13	10.11	63.63	10.39
17	84	33.7	446.62	$C_{24}H_{46}O_7$	64.54	10.38	64.86	10.63
				Z = S				
8	82	36.7	308.43	$C_{14}H_{28}O_5S$	54.51	9.15	54.83	9.22
10	86	32.1	336.49	$C_{16}H_{32}O_5S$	57.11	9.58	57.41	9.81
12	90	24.9	364.54	$C_{18}H_{36}O_5S$	59.30	9.95	59.75	10.06
14	96	26.4	392.59	$C_{20}H_{40}O_5S$	61.18	10.27	61.36	10.43
16	94	24.7	420.65	$C_{22}H_{44}O_5S$	62.81	10.54	63.05	10.69
18	91	23.1	448.70	$C_{24}H_{48}O_5S$	64.24	10.78	64.49	10.96
				Z = OC_3H_6S				
8	75	28.1	366.51	$C_{17}H_{34}O_6S$	55.71	9.35	55.59	9.52
10	78	27.4	394.56	$C_{19}H_{38}O_6S$	57.84	9.70	58.30	9.97
12	80	23.5	422.62	$C_{21}H_{42}O_6S$	59.68	10.01	60.19	10.34
14	92	22.9	450.67	$C_{23}H_{46}O_6S$	61.29	10.28	61.84	10.63
16	88	24.3	478.72	$C_{25}H_{50}O_6S$	62.72	10.52	63.28	10.85
18	92	21.2	506.77	$C_{27}H_{54}O_6S$	63.99	10.74	64.94	11.19

[a] Starting from compounds (**4**).
[b] In pyridine; *c* = 1; after a week.

Table 4. ^{1}H NMR chemical shifts for the 6-*Z*-*n*-alkyl-α-D-galactopyranoses (**5**) in $(CD_3)_2SO$ at 300 K.

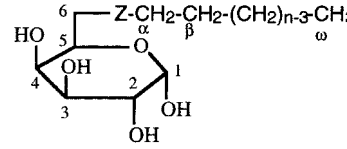

Site	Z = OCO		Z = S		Z = O–CH_2–CH_2–CH_2–S (1′ 2′ 3′)	
	δ/ppm	*J*/Hz	δ/ppm	*J*/Hz	δ/ppm	*J*/Hz
H1	4.93 (d)	$J_{1,2} = 3.15$	4.88 (t)	$J_{1,2} = 3.71$	4.91 (d)	$J_{1,2} = 2.98$
H2	3.50 (dd)	$J_{2,3} = 10.04$	3.50 (m)	$J_{2,3} = 6.78$	3.50 (dd)	$J_{2,3} = 7.48$
H3	3.55 (dd)	$J_{3,4} = 2.59$	3.52 (m)	$J_{3,4} = 2.00$	3.53 (dd)	$J_{3,4} = 2.90$
H4	3.65 (dd)	$J_{4,5} = 1.93$	3.71 (t)	$J_{4,5} = 0$	3.62 (d)	$J_{4,5} = 0$
H5	3.98 (m)	$J_{5,6} = 5.90$	3.85 (t)	$J_{5,6} = 6.27$	3.91 (t)	$J_{5,6} = 5.79$
H6a	4.05 (dd)	$J_{6a,6b} = 5.31$	2.65 (dd)	$J_{6a,6b} = 13.77$	3.40 (dd)	$J_{6a,6b} = 9.38$
H6b	4.05 (dd)	—	2.52 (dd)	—	3.36 (dd)	—
					H1′: 3.38 (t)	$J_{1',2'} = 6.72$
Z	—	—	—	—	H2′: 1.71 (q)	—
					H3′: 2.51 (t)	$J_{2',3'} = 6.39$
α-CH_2	2.26 (t)	$J_{\alpha\beta} = 7.32$	2.48 (t)	$J_{\alpha\beta} = 7.48$	2.44 (t)	$J_{\alpha\beta} = 6.39$
β-CH_2	1.50 (m)	/	1.49 (q)	—	1.49 (q)	—
(*n*-3)-CH_2	1.23 (s)	/	1.23 (s)	—	1.24 (s)	—
ω-CH_3	0.85 (t)	$J_{\omega,\omega-1} = 6.10$	0.85 (t)	$J_{\omega,\omega-1} = 6.10$	0.85 (t)	$J_{\omega,\omega-1} = 6.73$

ether. The yields, optical rotation and combustion analyses for these final compounds are given in table 3. The ^{1}H and ^{13}C NMR data are collated in tables 4 and 5, respectively.

Table 5. ^{13}C NMR chemical shifts δ (ppm) for the 6-*Z*-*n*-alkyl-α-D-galactopyranoses (**5**) in $(CD_3)_2SO$ at 300 K.

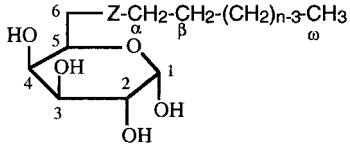

Site	Z = OCO	Z = S	Z = O–CH_2–CH_2–CH_2–S (1′ 2′ 3′)
C1	92.5	92.6	92.5
C2	68.4	69.3	68.5
C3	68.9	69.3	69.1
C4	69.1	69.2	69.3
C5	67.5	68.4	68.3
C6	63.7	31.7	70.1
			C1′: 68.9
Z	CO: 174.4	—	C2′: 29.3
			C3′: 28.1
α-CH_2	33.3	31.8	31.2
β-CH_2	24.3	31.2	31.0
(*n*-3)-CH_2	21.9–31.2	22.0–29.1	22.0–29.0
ω-CH_3	13.7	13.8	13.6

We gratefully acknowledge the EPSRC for support of an Advanced Fellowship (SMK). We would also like to thank the co-sponsored Alliance Program of the British Council and the Ministère des Affaires Etrangères, Direction de la Cooperation Scientifiques et Techniques for financial support for this research work. Mrs. J. Welsh and C. Kennedy (CHN) are also thanked for their technical assistance. Dr B. U. Komanschek at Daresbury Laboratories is thanked for his support and help.

References

[1] Andree, H., and Middehauve, B., 1991, *Tenside Surf. Det.*, **28,** 413.
[2] Balzer, D., 1991, *Tenside Surf. Det.*, **28,** 419.
[3] Hill, K., 1993, in *Carbohydrates as Raw Materials II*, edited by G. Descotes (VCH: Weinheim), p. 163 and references therein.
[4] Thomson, T. E., and Baron., A., 1975, *Biochim. Biophys. Acta*, **382,** 276.
[5] Diesenhofer, J., and Michel, H., 1989, *Angew. Chem.*, **101,** 872.
[6] Gregoriadis, J., Senior, J., and Poste, G. (editors), 1986, *Targeting of Drugs with Synthetic Systems* (New York: Plenum Press) and references therein.
[7] Lawrence, M. J., 1994, *Chem. Soc. Rev.*, 417.
[8] Lederer, E., 1976, *Chem. Phys. Lipids*, **16,** 91.
[9] Asselineau, D., and Asselineau, J., 1978, *Prog. Chem. Fats*, **16,** 59.
[10] Arita, H., Sugita, K., Nomura, A., Sato, K., and Kawanami, J., 1978, *Carbohydr. Res.*, **62,** 143.

[11] Riess, J. G., and Greomer, J., 1993, in *Carbohydrates as Raw Materials II*, edited by G. Descotes (VCH: Weinheim), p. 209 and references therein.
[12] Lesoal, T., Waszloewoez, I., and Nowak, J., 1980, *J. prakt. Chem.*, **322,** 877.
[13] Goodby, J. W., Haley, J. A., Mackenzie, G., Watson, M. J., Plusquellec, D., and Ferrieres, V., 1995, *J. mater. Chem.*, **5,** 2209.
[14] Goodby, J. W., Haley, J. A., Mackenzie, G., Watson, M. J., Kelly, S. M., Letellier, P., Douillet, O., Gode, P., Goethals, G., Ronco, G., and Villa, V., 1997, *Liq. Cryst.*, **22,** 367.
[15] Goodby, J. W., Haley, J. A., Mackenzie, G., Watson, M. J., Kelly, S. M., Letellier, P., Gode, P., Goethals, G., Harmouch, B., Martin, P., Ronco, G., and Villa, V., 1997, *Liq. Cryst.*, **22,** 497.
[16] Letellier, P., Ewing, D. F., Goodby, J. W., Haley, J., Kelly, S. M., and Mackenzie, G., 1997, *Liq. Cryst.*, **22,** 609.
[17] Miethchen, R., and Prade, H., 1994, *Carbohydr. Lett.*, **1,** 19.
[18] Prade, H., Miethchen, R., and Vill, V., 1995, *J. prakt. Chem.*, **337,** 427.
[19] Stangier, P., Vill, V., Rohde, S., Jeschke U., and Thiem, J., 1994, *Liq. Cryst.*, **17,** 589.
[20] Tietze, L. F., Böge, K., and Vill, V., 1994, *Chem. Ber.*, **127,** 1065.
[21] Jeffrey, G. A., 1984, *Mol. Cryst. liq. Cryst.*, **110,** 221.
[22] Tschierske, C., Lunow, A., and Zaschke, H., 1990, *Liq. Cryst.*, **8,** 885.
[23] Joachimi, D., Tschierske, C., Müller, H., Wendorff, J. H., Schneider, L., and Kleppinger, R., 1993, *Angew. Chem., int. Ed. Eng.*, **32,** 1165.
[24] Vill, V., Böcker, T., Thiem, J., and Fischer, F., 1989, *Liq. Cryst.*, **6,** 349.
[25] Jeschke, U., Vogel, C., Vill, V., and Fischer, H., 1995, *J. mater. Chem.*, **5,** 2073.
[26] Vill, V., Saierbrei, B., Fischer, H., and Thiem, J., 1992, *Liq. Cryst.*, **11,** 949.
[27] Bault, P., Gode, P., Goethals, G., Goodby, J. W., Haley, J. A., Kelly, S. M., Mehl, G. H., Ronco, G., and Villa, P., 1998, *Liq. Cryst.*, **24,** 283.
[28] Havlinova, B., Zemanovic, K., and Blazej, A., 1978, *Tenside Surf. Det.*, **15,** 119.
[29] Böcker, T., and Thiem, J., 1989, *Tenside Surf. Det.*, **26,** 318.
[30] Van Doren, H. A., Van der Geest, R., de Ruijer, C. F., Kellogg, R. M., and Wynberg, H., 1990, *Liq. Cryst.*, **8,** 109.
[31] Pfannemüller, B., and Welte, W., 1985, *Chem. Phys. Lipids.*, **37,** 227.
[32] Regnault, I., Ronco, G., and Villa, P., 1989, FR. Pat. No. 15 995, Générale Sucrière.
[33] Van Doren., H. A., and Wingert, L. M., 1994, *Recl. Trav. Chim. Pays-Bas*, **113,** 260.
[34] Kelly, S. M. and Füneschilling, J., 1994, *J. mater. Chem.*, **4,** 1673.
[35] Bras, W., Derbyshire, G. E., Bogg, D., Ekell, N. J., Komanschek, B. U., Naylor, S., and Ryan, A. J., 1995, *Science*, **267,** 996.
[36] Bras, W., and Boustra, J. A., 1993, *NIMPR*, **A326**, 587.
[37] Towns-Andrews, E., Berry, A., Bordas, J. G. Mant, R., Murray, P. K., Roberts, K., Sumner, I., Worgan, J. S., Lewis, R., and Gabriel, A., 1989, *Rev. Sci. Instrum.*, **60,** 2346.
[38] Folkhard, W., Geercken, W., Knoerzer, E., Mosler, E., Nemetschek-Gansler, H., Nemetschek, T., and Koch, M. H. J., 1987, *J. Mol. Biol.*, **193,** 405.